

A lateral model parameter correlation procedure for one-dimensional inverse modelling

Niels B. Christensen^{1*} and Rasmus J. Tølbøll²

¹Department of Earth Sciences, University of Aarhus, Høegh-Guldbergs Gade 2, 8000 Aarhus C, Denmark, and ²Mærsk Oil and Gas, Esplanaden 50, 1363 Copenhagen K, Denmark

Received February 2008, revision accepted September 2008

ABSTRACT

We present a new, fast and versatile method, the lateral parameter correlation method, of invoking lateral smoothness in model sections of one-dimensional (1D) models. Modern, continuous electrical and electromagnetic methods are capable of recording very large data sets and except for a few cases, standard inversion methodology still relies on 1D models. In environments where the lateral rate of change of resistivity is small, 1D inversion can be justified but model sections of concatenated 1D models do not necessarily display the expected lateral smoothness.

The lateral parameter correlation method has three steps. First, all sounding data are inverted individually. Next, a laterally smooth version of each model parameter, one at a time, is found by solving a simple constrained inversion problem. Identity is postulated between the uncorrelated and correlated parameters and the equations are solved including a model covariance matrix. As a last step, all sounding data are inverted again to produce models that better fit the data, now subject to constraints by including the correlated parameter values as *a priori* values. Because the method separates the inversion from the correlation it is much faster than methods where the inversion and correlation are solved simultaneously, typically with a factor of 200–500.

Theoretical examples show that the method produces laterally smooth model sections where the main influence comes from the well-determined parameters in such a way that problems with equivalence and poor resolution are alleviated. A field example is presented, demonstrating the improved resolution obtained with the lateral parameter correlation method. The method is very flexible and is capable of coupling models from inversion of different data types and information from boreholes.

INTRODUCTION

Over the past half a century, electrical and electromagnetic methods have been used to solve a huge variety of environmental and hydrogeophysical problems (Fitterman 1987; Sandberg and Hall 1990; Taylor, Widmer and Chesley 1992; Albouy *et al.* 2001; Sørensen *et al.* 2005; Auken *et al.* 2006). More and more, single-site applications of various methods have given way to the use of continuous, measure-while-moving methods, both ground based and airborne and it has

become economically possible to investigate extensive areas with fairly dense coverage. Among the continuous geoelectrical methods can be mentioned multi-electrode systems for DC resistivity measurements (Dahlin 1996; Bernstone and Dahlin 1999) and the pulled-array continuous electrical sounding (PACES) system (Sørensen 1996) and others (Panissod, Lajarthe and Tabbagh 1997). Airborne systems in both frequency and time-domain, today often helicopter-borne, are finding increased use. The frequency domain HEM method (Sengpiel and Siemon 2000; Siemon 2001; Tølbøll and Christensen 2006) and airborne transient systems (Balch *et al.* 2002; Eaton *et al.* 2002), including the recent SkyTEM system

*E-mail: nbc@geo.au.dk

(Sørensen and Auken 2004), have been used in hydrogeophysical investigations to map deep, buried valley aquifers, salt water intrusion, capping clays, etc. A general characteristic of continuous methods is that they produce very large data sets and quantitative inversion of the data becomes time consuming.

For a number of reasons, inversion of electrical and electromagnetic data still relies on 1D models to a large extent. First of all, inversion with 1D models is considerably faster than multidimensional inversion and for large data sets computation time is an issue even with modern computers. Secondly, a 1D formulation can be justified if the lateral rate of change of the subsurface resistivity is small, which is often the case in layered sedimentary environments. Thirdly, inversion programs for full non-linear 2D inversion, not to speak of 3D inversion, are simply not commercially available for some data types, e.g. airborne frequency and time-domain data. Fourthly, even if they are, as is the case for geoelectrical data, most of them employ finely discretized models in a regularized inversion, resulting in smooth minimum-structure models without sharp boundaries between formation boundaries (Oldenburg and Li 1994; Loke and Barker 1996; Loke, Acworth and Dahlin 2003). Exceptions are the method presented by Smith *et al.* (1999) and by Auken and Christiansen (2004) who developed a sharp boundary 2D inversion for plane wave and geoelectrical data, respectively. Olayinka and Yaramanci (2000) presented a method for 2D inversion of DC resistivity data using a set of rectangular blocks of homogeneous resistivity.

The use of 1D inversion techniques for interpretation of sounding data is of course not unproblematic. The individually inverted models are likely to suffer from the influence of 2D and 3D structures and even when the 1D assumption is justified, model sections of concatenated 1D models do not necessarily display much of the expected lateral smoothness. The challenge is therefore to develop a method that combines the use of the conventional 1D formulation with lateral continuity in a quantitative manner. The method should, as a minimum, allow for the inclusion of different data types and provide a sensitivity analysis of the model parameter resolution.

Different techniques invoking lateral smoothness of 1D model sections have been published in the literature: Gyulai and Ormos (1999) presented a procedure for interpretation of DC resistivity data using 1D models. Lateral model continuity is ensured by expressing the model parameters through laterally slowly-varying functions expanded into power or harmonic function series and by solving the inversion problem in terms of the coefficient of the expansion. Another approach was described by Santos (2004), who used a 2D roughness matrix with 1D models to produce laterally smooth models.

Auken *et al.* (2005) suggested a laterally constrained inversion procedure that simultaneously solves for all 1D models, including lateral constraints on any number of model parameters and model parameter combinations. The output models are accompanied by a comprehensive sensitivity analysis of the model parameter resolution that includes the effect of the applied lateral constraints. Recently, Brodie and Sambridge (2006) have presented the 'holistic inversion' concept in which inversion is carried out on both model parameters and configuration and calibration parameters. For every parameter, a regular 2D rectangular grid is defined and the value of model parameters is defined by their node values. The node values are found by expressing the parameter values at the measuring points as spline coefficients relating to the node points and by simultaneously inverting all data sets.

The dilemma of 1D inversion of large data sets is that:

- 1 fitting the data with individual models will often produce model sections that are geologically unlikely;
- 2 invoking lateral smoothness by expressing the model parameters through functions defined by a fairly small set of parameters will not permit complexity where it is in fact resolved (Gyulai and Ormos 1999; and – to a certain extent – Brodie and Sambridge 2006);
- 3 full, simultaneous inversion of a large number of data sets can become computationally very heavy (Auken *et al.* 2005).

In the following sections we will present a new method for obtaining laterally smoothly varying 1D models which we have named: the lateral parameter correlation method. The method is of an iterative nature, separating the 1D inversions from the lateral correlation. Initially, all soundings are inverted individually with 1D models, all with the same number of layers. Subsequently, the lateral correlation is carried out on the model parameters, one at a time. A laterally smooth version of each parameter is found by solving a simple inversion problem. Identity is postulated between the model parameters of the initial inversion and the smooth version and the equations are solved including a model covariance matrix. The *a posteriori* model covariance matrix of the inversion problem of the correlation provides uncertainty estimates of the correlated parameters. As a last step, all sounding data are inverted again, now subject to constraints by including the correlated parameter values as prior values with an uncertainty equal to the uncertainty estimate on the correlated values.

1D INVERSION OF EM DATA

There are numerous approaches to the inversion of EM data with a 1D model consisting of horizontal, homogeneous and isotropic layers. The one we shall refer to in this paper is

a well-established iterative damped approach (Menke 1989). Formally, the model update at the n -th iteration is given by

$$\mathbf{m}_{n+1} = \mathbf{m}_n + [\mathbf{G}_n^T \mathbf{C}_{obs}^{-1} \mathbf{G}_n + \mathbf{C}_{prior}^{-1} + \mathbf{R}^T \mathbf{C}_R^{-1} \mathbf{R} + \lambda \mathbf{I}]^{-1} \cdot \left[\mathbf{G}_n^T \mathbf{C}_{obs}^{-1} (\mathbf{d}_{obs} - \mathbf{g}(\mathbf{m}_n)) + \mathbf{C}_{prior}^{-1} (\mathbf{m}_{prior} - \mathbf{m}_n) + \mathbf{R}^T \mathbf{C}_R^{-1} (-\mathbf{R} \mathbf{m}_n) \right] \quad (1)$$

where \mathbf{m} is the model vector containing the logarithm of the model parameters, \mathbf{G}_n is the Jacobian matrix containing the derivatives of the data with respect to the model parameters, T is the vector transpose (and conjugate, if complex), \mathbf{C}_{obs} is the data error covariance matrix, \mathbf{C}_{prior} is the covariance matrix of the prior model, \mathbf{R} is the roughening matrix containing 1s and -1 s for the constrained parameters and 0s at all other places, \mathbf{C}_R is the covariance matrix describing the strength of the correlation constraint, λ is the Marquard damping factor, \mathbf{I} is the identity matrix, \mathbf{d}_{obs} is the field data vector, $\mathbf{g}(\mathbf{m}_n)$ is the nonlinear forward response vector of the n -th model and \mathbf{m}_{prior} is the prior model vector. In this study, as in most other works, the data noise is assumed to be uncorrelated, implying that \mathbf{C}_{obs} is a diagonal matrix.

1D inversion is carried out with both few-layer and multi-layer models. In the few-layer inversion, the layer resistivities and the thicknesses are free to vary and no constraints are applied to combinations of model parameters, corresponding to an exclusion of the \mathbf{R} -term in equation (1). Generally, the few-layer inversion aims at minimizing the data misfit using a specific, small amount of layers. In the multi-layer inversion, the layer boundaries are totally fixed and only the layer resistivities are free parameters. The inversion is regularized through vertical constraints – the \mathbf{R} -term in equation (1) – ensuring identity between neighbouring layer resistivities within a given relative uncertainty.

The model parameter uncertainty estimate relies on a linear approximation to the posterior covariance matrix, \mathbf{C}_{est} , given by

$$\mathbf{C}_{est} = [\mathbf{G}^T \mathbf{C}_{obs}^{-1} \mathbf{G} + \mathbf{C}_{prior}^{-1} + \mathbf{R}^T \mathbf{C}_R^{-1} \mathbf{R}]^{-1} \quad (2)$$

where \mathbf{G} is based on the final model. The analysis is given by the standard deviations of the model parameters, obtained as the squareroot of the diagonal elements of \mathbf{C}_{est} (e.g. Inman, Ryu and Ward 1975).

THE LATERAL PARAMETER CORRELATION METHOD

In the following section, a quick overview is given of the LPC methodology. More details and a deeper discussion are given

in the subsequent section. The lateral parameter correlation method consists in the following three steps:

1 Individual inversion: the first step is to invert the soundings in the ordinary uncorrelated way. The LPC method is then applied to the individually inverted models.

2 Lateral correlation: having obtained the individually inverted models, the correlation is carried out on the model parameters, one at a time. Correlation can be done not only on the model parameters: layer resistivities and layer thicknesses but also on depths to layer boundaries. The values of the selected parameter for all models are collected in the parameter vector \mathbf{p} . The correlation is formulated as a constrained inversion problem where \mathbf{p} plays the role of the data vector and the model vector that we wish to find, \mathbf{p}_{cor} , is a smoother version of \mathbf{p} . The forward mapping between \mathbf{p} and \mathbf{p}_{cor} is given by

$$\mathbf{p} = \mathbf{I} \mathbf{p}_{cor} + \mathbf{e} \quad (3)$$

where \mathbf{I} is the identity matrix and \mathbf{e} is the observational error. The smoothing is realized by inverting the above relationship incorporating a model covariance matrix, \mathbf{C}_m , containing the elements

$$C_m^{i,j} = \sigma_0^2 \exp(-r_{i,j}) \quad (4)$$

where $r_{i,j}$ is the normalized distance between the i -th and the j -th model position and σ_0 is the standard deviation of the correlation for the model parameter in question. The normalized distance is defined by

$$r_{i,j} = \sqrt{\left(\frac{x_i - x_j}{L_x}\right)^2 + \left(\frac{y_i - y_j}{L_y}\right)^2} \quad (5)$$

where L_x and L_y are the correlation lengths in the x - and y -directions, respectively. Applying no other constraints to \mathbf{p}_{cor} , the solution of equation (3) can be formulated as:

$$\mathbf{p}_{cor} = (\mathbf{I}^T \mathbf{C}_p^{-1} \mathbf{I} + \mathbf{C}_m^{-1})^{-1} \mathbf{I}^T \mathbf{C}_p^{-1} \mathbf{p} = (\mathbf{C}_p^{-1} + \mathbf{C}_m^{-1})^{-1} \mathbf{C}_p^{-1} \mathbf{p} \quad (6)$$

\mathbf{C}_p is a diagonal error covariance matrix of the uncorrelated parameters. Its elements are the variances of the parameters of the uncorrelated models, i.e., it is built from the diagonal elements of the posterior covariance matrices of the individual inversions for the pertinent parameter, \mathbf{C}_{est} , in equation (2). The standard deviations of the correlated model parameters, \mathbf{p}_{cor} , are finally found as the squareroot of the diagonal elements of the linear approximation to the posterior covariance matrix \mathbf{C}_{est}^{lpc} given as

$$\mathbf{C}_{est}^{lpc} = (\mathbf{C}_p^{-1} + \mathbf{C}_m^{-1})^{-1} \quad (7)$$

3 Final inversion: as a consequence of the smoothing involved in the correlation process, the correlated models do not generally fit the data as well as the uncorrelated models. To remedy this without giving up the smoothness of the correlated models, a subsequent constrained inversion of the field data is performed with the correlated values p_{cor} as *a priori* values on the model parameters, the m_{prior} vector of equation (1). The covariance matrix of the *a priori* values, the C_{prior} of equation (2), is taken to be diagonal, i.e., there is no cross correlation between the laterally correlated parameters and it is defined by the variance of the correlated model parameters, i.e., $C_{prior} = \text{diag}(C_{est}^{lpc})$.

Let us consider each step in more detail.

The individual inversions

Normal care should be taken in the individual inversions in terms of defining a proper data error covariance matrix and ensuring convergence of the inversion. *A priori* information can be included in the inversion at this stage but it is most often better to save it for the LPC procedure.

The lateral correlation

It is clear that the lateral parameter correlation method can only be applied to models having the same number of layers.

The standard deviation of the correlation, i.e., the value of σ_0 in equation (4), should reflect the statistics of the geological variability of the area. However, quantitative information on the geological variability is often very limited, if existing at all and the value of the standard deviation of the correlation for the different model parameters must therefore be determined pragmatically and/or on the basis of theoretical modelling experiments. The correlation lengths, L_x and L_y , should generally be chosen a few times the largest distance between any model positions in the considered area. This ensures that – in principle – all parameters are correlated with all other parameters which is a reasonable initial hypothesis.

The C_m matrix needs to be calculated only once for every data set to be correlated; it is purely geometrical and is the same for all model parameters. However, the standard deviation of the correlation, σ_0 , is in general different for every model parameter.

Since the lateral parameter correlation procedure is performed on one model parameter at a time, it is basically up to the interpreter to determine which model parameters to include in the correlation. Generally, lateral constraints will be included on both layer resistivities and thicknesses

or depths to layer boundaries. Correlation of depths to layer boundaries is often preferable to correlation on layer thicknesses because continuity of depths is more relevant when considering a layered, sedimentary environment (Auken *et al.* 2005). However, correlation on layer depths may result in intersecting layer boundaries. In this case, a minimum layer thickness must be invoked and a choice between the lower or upper value of the depth to the layer boundary must be made.

Most often, inversion of electromagnetic data is performed on the logarithm of the model parameters, partly to ensure positivity and partly to make the inversion problem less non-linear. As a consequence, C_{est} of equation (2) will contain the variance and covariance of the logarithm of the model parameters: resistivities and thicknesses. Normally, it would be appropriate to correlate the logarithm of resistivities but it can be argued that the correlation of depths/thicknesses should be done linearly, since the vertical variability of the layer boundaries is normally expected to be the same at any depth. While the variance of the logarithm of resistivities needed for the C_p matrix of equation (6) is readily available from C_{est} , we need to estimate the variance of linear thickness, t and depth, d , from the variance and covariance of their logarithm given in C_{est} . Using that $\text{var}[f(x)] \approx [f'(x)]^2 \text{var}(x)$ is correct to the first order, we find

$$\text{var}(t) \approx t \text{var}(\ln t) \quad (8)$$

$$\begin{aligned} \text{var}(d_k) &= \text{var}(t_1 + t_2 + \dots + t_k) = \sum_{i=1}^k \sum_{j=1}^k \text{covar}(t_i, t_j) \\ &\approx \sum_{i=1}^k \sum_{j=1}^k t_i t_j \text{covar}(\ln t_i, \ln t_j) \end{aligned} \quad (9)$$

The above method of lateral correlation of inverted models does not depend on data lying on a straight line or being equidistant because the model covariance matrix is based on the lateral distance between the models. It is also possible to correlate models obtained by inversion of different data types and to incorporate information from other sources, e.g., drill hole information, as long as it can be formulated in terms of a model (Tølbøll 2007).

As can be seen from equation (6), the matrices to be inverted are full and for large data sets the inversion problem of the correlation can become quite large and the solution thereby time-consuming. This is, however, easily remedied by dividing the data set into smaller, overlapping segments of appropriate size.

The final, constrained inversion

The final inversion with the correlated parameters as *a priori* constraints serves to strike a compromise between laterally smoothly varying models and models that will fit the data well. The inversion is started with the final model of the individual inversions as initial models and includes the smooth parameter values as *a priori* values with their appropriate variances, so convergence is very fast and computation time negligible.

The model parameter uncertainty estimate of the final constrained inversion will in general be considerable smaller than for the individual inversions because of the inclusion of prior information from the correlated parameters. This reflects the improved determination invoked by the assumed lateral continuity.

THEORETICAL EXAMPLES

The synthetic data set used for the theoretical examples, is generated for a multi-electrode DC resistivity system with a unit electrode distance of 5 m configured to measure in a conventional Wenner electrode array with nine electrode distances of 5, 10, 15, 20, 30, 40, 60, 100 and 120 m.

The forward model, shown in Fig. 1(a), simulates a typical layered sedimentary environment with a clayey till layer underlain by resistive sand and heavy, well-conducting clay, respectively. The thickness of the embedded sand layer increases gradually along the profile from a few metres to more than 50 m, while the capping clay layer shows only moderate variations. The model is generated using a stationary stochastic process characterizing the spatial variability of the earth by von Karman covariance functions (Møller, Jacobsen and Christensen 2001; Serban and Jacobsen 2001). These functions enable the construction of complex layered models, which resemble sedimentary environments to a high degree. In the generation of the models as statistical realizations, average layer resistivities are 30, 80 and 10 Ωm from top to bottom and the standard deviations for all logarithmic layer resistivities are 0.5. Average layer thicknesses are 30 and 80 m for the two uppermost layers and the standard deviation on the thicknesses is equal to the mean value. Data are sampled every 5 m along the 700 m profile and 5% laterally uncorrelated, random noise is added to simulate a true data set. Only soundings located between coordinates 200 and 500 m, where the data coverage is complete, are included in the inversion. The forward calculations are performed using a 2D finite-difference code from University of British Columbia (McGillivray 1992) optimized with respect to the input model characteristics and

the applied electrode configurations. The location of two theoretical boreholes that will be used later are also shown in Fig. 1(a). The conventional data pseudosection with focus points is shown in Fig. 1(b). The focus depth is defined as half the Wenner electrode spacing (Edwards 1977).

Figure 1(c) clearly demonstrates that the true model section is poorly reproduced using a simple uncorrelated three-layer inversion approach, except for the capping clay layer that is close to the true model along the entire profile. In the profile interval 250–350 m and 425–500 m, the thickness of the embedded high-resistivity sand layer is overestimated, probably mostly due to poor depth resolution. Conversely, due to the presence of 2D effects in the data combined with high-resistivity equivalence, it is consistently severely underestimated between coordinates 350 and 425 m. At the beginning of the profile, between coordinate 200 and 250 m, the individual 1D models suffer from a lack of lateral continuity. In all cases, the poor model reproduction is supported by the model parameter uncertainty analysis, which indicates that e.g. both the resistivity and the thickness of the second layer are unresolved in the interval 350–425 m, while the underestimated resistivity appears well determined in the interval 425–500 m because the layer is thick and close to the surface.

Figure 1(d-f) shows the model section resulting from the lateral parameter correlation procedure (correlation plus final inversion) with three different correlation standard deviations of $\sigma_0 = 45, 14$ and 4.5 on the depths to layer boundaries, respectively. In all three cases, the correlation length along the profile is 1000 m and the layer resistivity correlation standard deviation is $\sigma_0 = 1.4$. Linear correlation is used for layer depths, while logarithmic correlation is used for layer resistivities. By comparison with Fig. 1(c), it appears that the embedded high-resistivity layer is considerably better reproduced in the correlated model sections compared to the uncorrelated model section. The artefacts caused by the high-resistivity equivalence are reduced and the model fluctuations in the first part of the profile, which are unlikely to reflect geological variations, are removed. It appears that a correlation standard deviation of $\sigma_0 = 14$ in this case provides the best fit to the true model.

The effect of the correlation step of the lateral parameter correlation procedure is illustrated in Fig. 1(g) where a section of the models obtained after the correlation but before the final inversion, is shown. The analysis shows the corresponding uncertainty of the model parameters and the plot of residuals shows the fit between the data and the forward responses of the correlated model section. Correlation standard deviations corresponding to the intermediate level in Figure 1e have been

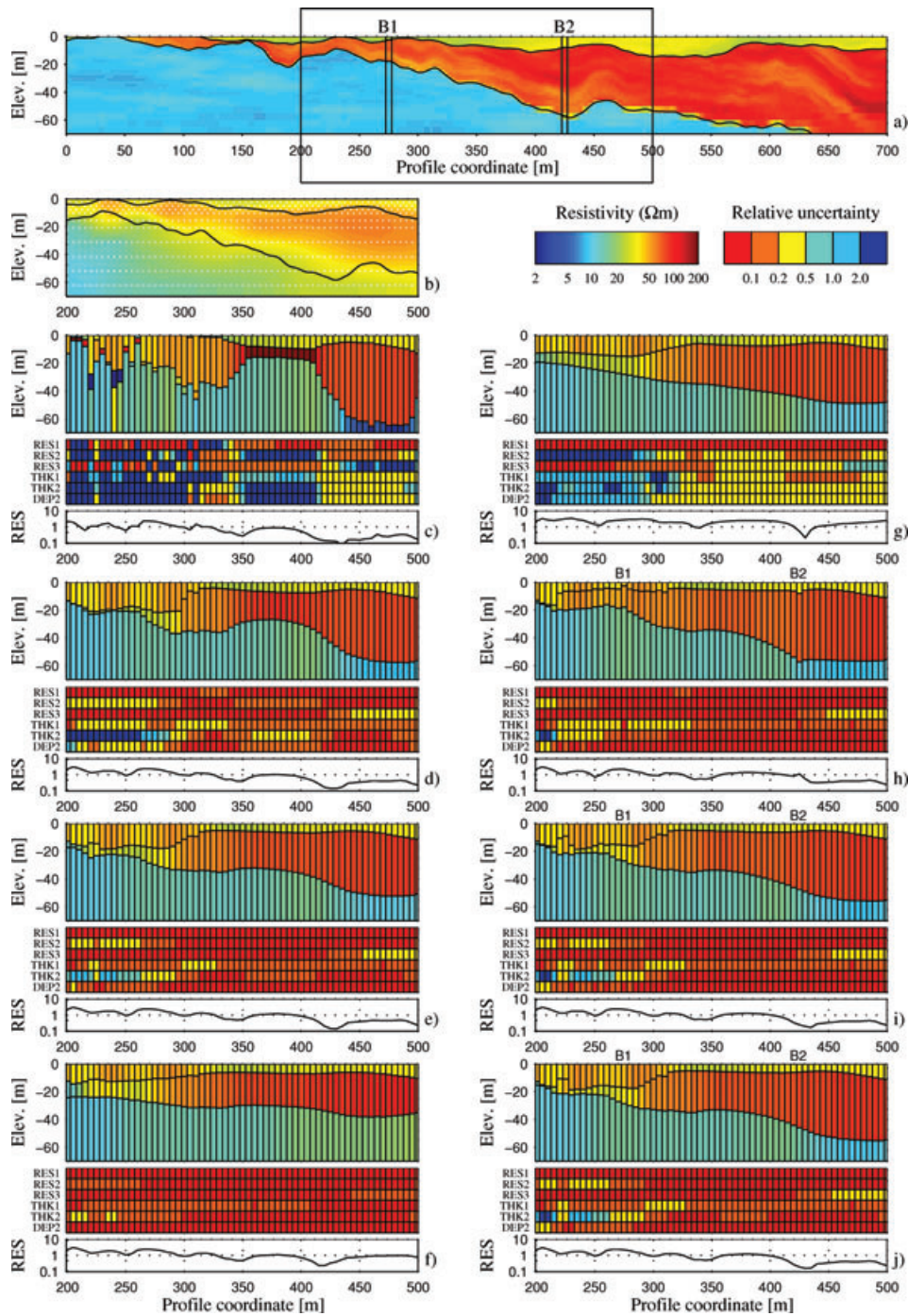


Figure 1 Synthetic multi-electrode DC resistivity example. (a) True model generated as a statistical realization using von Karman covariance functions with mean resistivity values (top to bottom) of 30, 80 and 10 Ωm . (b) Conventional data pseudosection with focus points as white dots. (c) Uncorrelated few-layer inversion result with analysis section and residuals. Only soundings between coordinate 200 m and 500 m with complete data coverage (the black box in Fig. 1a) are used for the inversion. In all the following plots, correlation lengths of 1000 m in both x - and y -directions and a correlation standard deviation of $\sigma_0 = 1.4$ on the logarithm of layer resistivities have been used. (d)–(f) lateral parameter correlation model sections obtained with three different linear correlation standard deviation on depth to layer boundaries: $\sigma_0 = 45, 14$ and 4.5 , respectively. (g) Model section after correlation but before final inversion for a correlation standard deviation of $\sigma_0 = 14$ on the depth to the layer boundaries. (h)–(j) Model sections as (e) but with borehole information included at profile coordinates 275 m and 425 m; in (h), the borehole is on the profile, in (i) and (j) the boreholes are 50 m and 100 m from the profile, respectively.

used. When comparing with the results after final inversion in Fig. 1(e), it is seen that the model section is overly smooth and that the residuals are higher. This illustrates that, by adjusting the models according to the data, the final inversion brings the residuals down to a level that is only insignificantly higher than for the uncorrelated inversion.

In Fig. 1(h-j), the lateral parameter correlation procedure includes supplementary information on the depth to the layer boundaries of the second layer from the two drill holes, B1 and B2, positioned at profile coordinates 275 m and 425 m. The borehole information is integrated in the lateral parameter correlation procedure by defining two models representing the boreholes with appropriate model parameter uncertainties. In this case, all model parameters are completely uncertain except the depths to the boundaries of the second layer. The two borehole models are included in the parameter vector, \mathbf{p} , of equation (3) before correlation and removed again from the smooth model vector, \mathbf{p}_{cor} , before the final inversion. All three correlations use the same setting as in Fig. 1(e) with a fixed depth correlation standard deviation of $\sigma_0 = 14$ but the projected distance from the drill hole to the profile (offset) is set to 0, 50 and 100 m in Fig. 1(h-j), respectively. Comparing with Fig. 1(e) it is immediately clear that the inclusion of the drill hole information leads to a somewhat better reproduction of the true model. As expected, the thickness of the high-resistivity layer is closer to the true value in the neighbourhood of the boreholes and the model parameter determination is generally improved. For a 50 m offset, Fig. 1(i), the effect of the supplementary drill hole is somewhat reduced and for a 100 m offset, Fig. 1(j), the effect is no longer significant.

FIELD EXAMPLE

In Tølbøll and Christensen (2006), the lateral parameter correlation method has been applied along profile lines on helicopterborne frequency domain electromagnetic (HEM) data. Furthermore, an example of combined lateral correlation of HEM profiles and borehole data is documented in Tølbøll (2007). Here we shall look at an example involving ground based radiomagnetotelluric data with areal coverage.

Our field example illustrates the use of the lateral parameter correlation method on data from a radiomagnetotelluric investigation in the Grundfør area, Denmark. The area is characterized by Quaternary sediments of sand and clay in the upper 100 m of the subsurface. Data were collected in 1995 in collaboration with Universität zu Köln, Institut für Geophysik und Meteorologie, Germany, with their RMT equipment that was developed by Imre Müller, Centre d'Hydrogéologie, Uni-

versité de Neuchâtel, Switzerland. The instrument measures scalar radiomagnetotelluric data at four frequencies: 16.8, 53.0, 126.8 and 183.0 kHz and soundings with the electric field in both the north-south and the east-west direction, were recorded. Here, only the data with the electric field in the north-south direction are used. The radiomagnetotelluric method, the instrument and the survey technique is described in Tezkan (1999) and Tezkan, Hördt and Gobashy (2000). Data were collected in a 200 m by 450 m area on 21 profile lines with typically 45 soundings per line. The line spacing was 10 m and soundings were made with a density of 10 m (a few with 5 m intervals) along the profiles, a total of 906 soundings.

Data were inverted with multi-layer models with 20 layers. The inversion was carried out using a L1-norm optimization which produces blocky models (Farquharson and Oldenburg 1998). Regularization was imposed by claiming identity between the log(resistivity) of neighbouring layers within an uncertainty of $\sigma_0 = 1.4$. Inspection of the model sections along the profiles showed that a 3-layer model would be adequate for few-layer inversion. Initial models for the 3-layer inversion were estimated from the 20 layer model (Tølbøll and Christensen 2006).

Computation time on a single-thread process, 2 GHz Pentium 4 CPU for the initial uncorrelated inversion was 30 s for the multi-layer models and 1.6 s for the 3-layer models. Correlation of the 20 layer resistivities of the multi-layer models took 158 s and 45 s for the 3-layer models. The final inversion required 30 s for the multi-layer models and 1.7 s for the 3-layer models. The second inversion thus took approximately the same time as the first uncorrelated inversion. This is uncommon and only happens because 1D radiomagnetotelluric inversion is so exceedingly fast.

Figs 2(a) and 2(c) present the uncorrelated inversion results of Line-10 traversing the centre of the area obtained using the multi-layer model and the 3-layer model, respectively, while Figs 2(b) and 2(d) show the correlated models. For the multi-layer models, a value of $\sigma_0 = 1.4$ was adopted for log(resistivities) while for the 3-layer model a value of $\sigma_0 = 1.0$ was used. Depths to layer boundaries in the 3-layer model were linearly correlated with values of $\sigma_0 = 1.4$ and $\sigma_0 = 14$ for the top and the bottom layer boundary, respectively. The uncorrelated multi-layer and 3-layer inversions are very similar, mostly due to the fact that a L1-norm was used in the multi-layer inversion, both for the initial and the final inversions. The correlated version of the multi-layer model section shows the expected lateral smoothness and it is also seen that smoothness increases with depth. This is due to the increasing uncertainty of the resistivities of

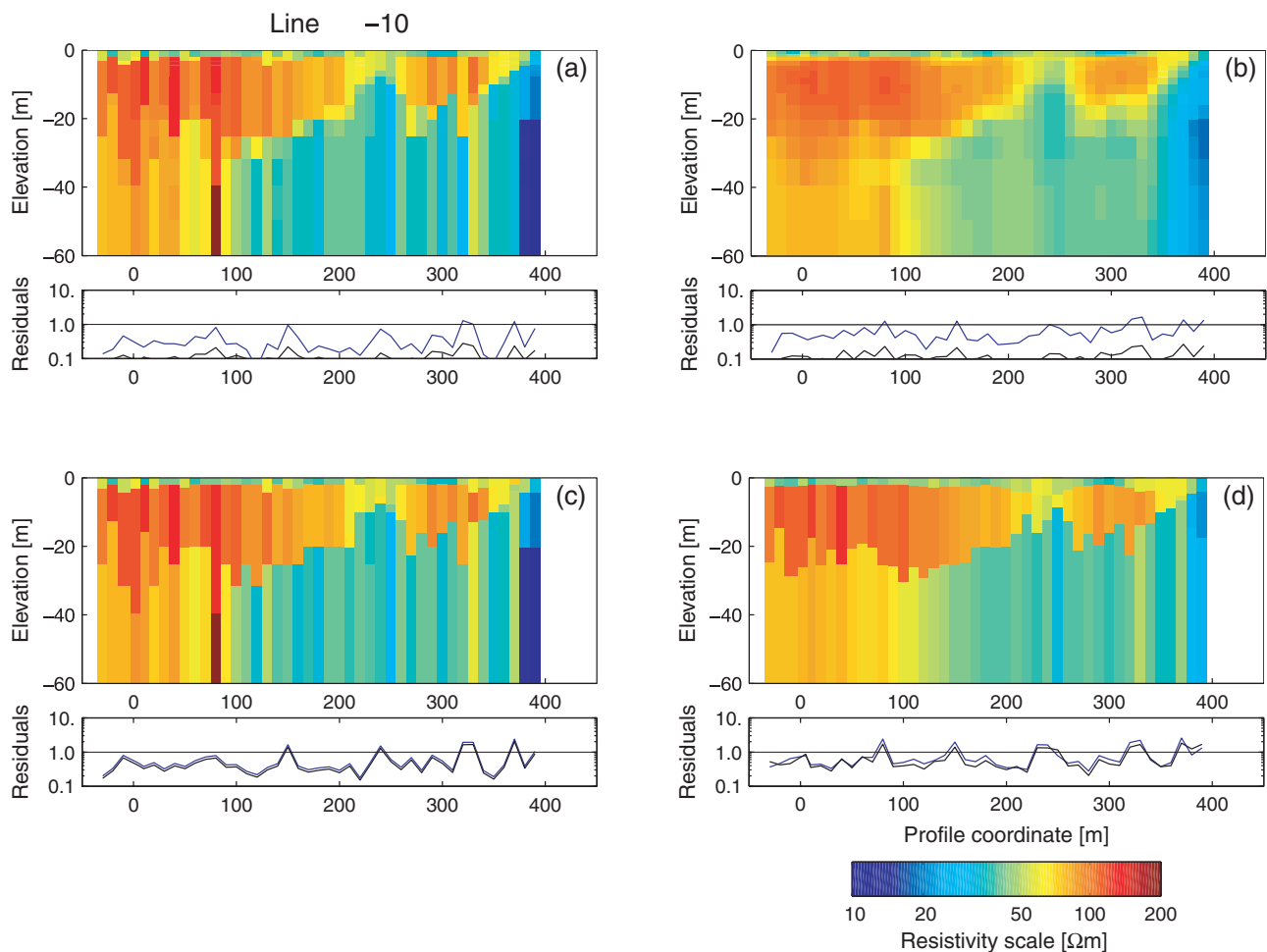


Figure 2 Model section for Line-10 from the inversion of the radiomagnetotelluric data from Grundfør, Denmark. (a) Uncorrelated multi-layer inversion result; (b) correlated multi-layer inversion result; (c) uncorrelated 3-layer inversion result; (d) correlated 3-layer inversion results. Log(resistivities) have been correlated with a value of $\sigma_0 = 1.4$ for the multi-layer models and $\sigma_0 = 1.0$ for the 3-layer models and depths to the layer boundaries in (d) have been linearly correlated with a value of $\sigma_0 = 1.4$ and $\sigma_0 = 14$ for the top and bottom boundary, respectively.

the deeper layers in the first uncorrelated inversion and the fact that the correlation is imposed with the same standard deviation for all layers. It is seen that the lateral smoothing also affects the final L1-norm inversion of the multi-layer models by making them less blocky than the initial L1-norm inversion. The correlated 3-layer model section also shows increased lateral smoothness but now displays approximately the same standard deviation for all layers because the uncertainty of the resistivities in the initial uncorrelated 3-layer inversion are of the same order of magnitude. Notice that for both multi- and few-layer inversions, the lateral correlation does not remove the more conductive feature at a depth of 10 m at profile coordinate 240 m. This is due to the fact that the resistivities of the initial inversion are well determined by data.

All model sections in Fig. 2 show a top layer with a thickness of ≈ 2 m and a resistivity of $\approx 50 \Omega\text{m}$: a clayey moraine till. The second layer is a high resistivity layer of 100–200 Ωm and a thickness of 15–30 m: a sandy formation. The bottom segment has resistivities of 40–70 Ωm : a sandy formation with more fine grained material.

To further illustrate the effect of the lateral correlation, contoured maps of the mean resistivity in the depth interval 2–5 m are shown in Fig. 3(a–c) calculated from the 3-layer models. In Fig. 3(a), the mean resistivity is based on the uncorrelated models of the initial inversion. In Fig. 3(b), the mean resistivity is based on the models obtained from correlation only along profile lines and in Fig. 3(c) it is based on models resulting from correlation in the entire plane. Naturally, the maps created based on the correlated models in Figs 3(b) and 3(c)

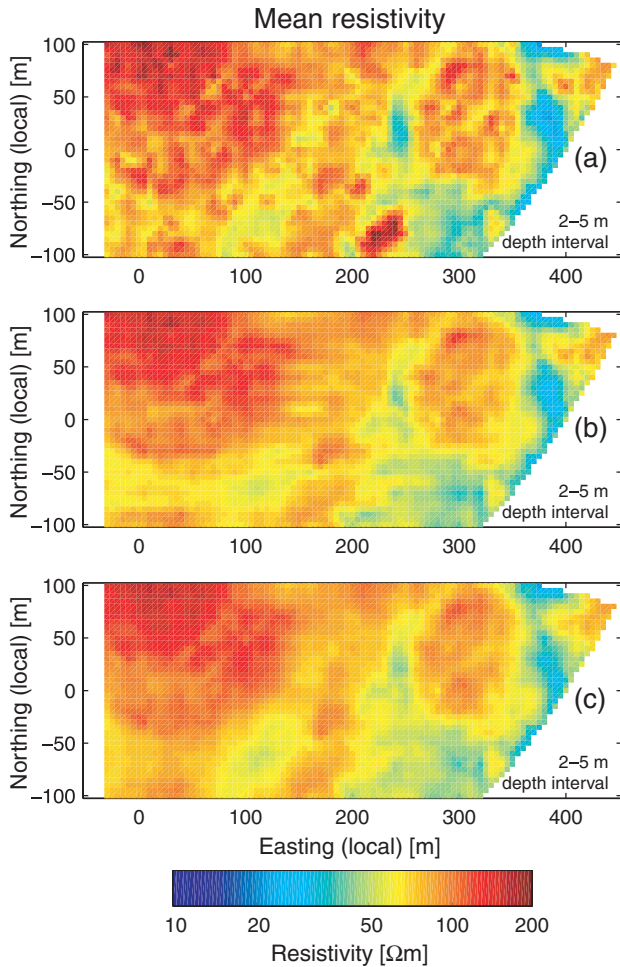


Figure 3 Contoured map of the mean resistivity in the depth interval 2–5 m based on the 3-layer models. (a) Uncorrelated 3-layer models; (b) 3-layer models correlated only along the profile lines; and (c) 3-layer models from the entire survey correlated in the plane.

appear smoother. Note, however, that the sandy area at easting coordinate 250 to 350 m and northing coordinate -30 to 100 m framed by clay retains its clear definition, also in the case of correlated models. The feature shown in this depth interval is found almost identically for depth intervals down to 20 m depth (not shown) and shows a sand body framed by clayey material. The importance of correlating not only along profile lines, but in the entire plane, can be seen by comparing Figs 3(b) and 3(c). In Fig. 3(b), correlation is done only along the horizontal profiles while Fig. 3(c) shows the same map, now created with correlation in the entire plane. Even with a data set as regularly spaced and dense as the one shown here, it is apparent that correlation only along profile lines gives a striped character to the map in certain places while the map

resulting from correlation in the entire plane does not show preferential direction. For more sparse and irregular data sets, the advantage of correlating in the entire plane would be even more obvious.

DISCUSSION

The fundamental characteristic of the lateral parameter correlation method is that it separates the inversion from the lateral correlation. This makes the method much faster than other methods of lateral correlation relying on a simultaneous inversion of a large number of soundings including lateral constraint in every iterative step. In typical applications, the number of model parameters in the 1D model is much smaller than the number of models and in the lateral parameter correlation approach, there will only be as many large-scale inversions as there are model parameters – plus one to invert the model covariance matrix C_m^{-1} of equation (6). The computation time for the final inversions is negligible because they are initialized with the results of the individual inversion.

Let us assume that we have N data sets, each to be inverted with 1D models with P parameters and that NIT iterations are needed for convergence. Let us also assume that the computation time for matrix inversion is proportional to the cube of the matrix size. Then the computation time for the simultaneous inversion methods will be $\propto (P \cdot N)^3 \cdot NIT$. For the present lateral parameter correlation method, the computation time will be $\propto [P^3 \cdot N \cdot NIT + (P + 1) \cdot N^3 + P^3 \cdot N \cdot NIT2]$, where the first term is the time used for the initial uncorrelated 1D inversion, the second term is the time used in the lateral correlation procedure and the last term is the time used for the final 1D inversion. $NIT2$ is the number of iterations in the final 1D inversion and is considerably smaller than NIT . Evidently, the second term, $(P + 1) \cdot N^3$, is dominating in the lateral parameter correlation procedure, so the ratio between computation times is $R \approx [(P \cdot N)^3 \cdot NIT] / [(P + 1) \cdot N^3] \approx P^2 \cdot NIT$. Assuming $NIT = 10$, we have for a 20-layer multi-layer model: $R = 4,000$. For 3-layer models there are 5 model parameters and we have: $R = 250$; for 4-layer models we get $R = 490$. For very large surveys, the inversion problem of the correlation can be segmented into overlapping regions to reduce computation time.

The fact that the data inversion and the correlation are separated means that the correlation takes place exclusively in the model space which makes it easy to correlate models from different methods: parameters from all the methods are just concatenated in the construction of the p vector and the C_p matrix. It also makes it easy to include information from other

sources, e.g. resistivity levels or the depth to layer boundaries from logs in boreholes. After the correlation, the correlated parameters and their variances will just have to be separated again and included in the final data inversion of each method.

As shown in the second example (see Fig. 3), it is important to be able to correlate data sets with areal coverage over the entire area and not just along profile lines. The lateral parameter correlation approach does not require data to be along profiles; the mathematical formulation does not distinguish between areal and profile oriented correlation.

The price paid for the separation of the inversion and the correlation is that cross-correlation information between the model parameters of the individual inversions is discarded. Only the diagonal elements of the individual posterior covariance matrices are assembled to form the data error covariance matrix of the correlation inversion – the C_p matrix of equation (6). If data errors are laterally correlated, e.g., from dimensionality effects, the uncertainty of the model parameters will also be laterally correlated. However, in the lateral correlation procedure we assume that the errors on the parameters (now as data in the lateral correlation procedure) are uncorrelated. The effect of this is that the posterior uncertainty of the correlated parameters will be underestimated. After the correlation problem has been solved, the covariance matrix of the prior parameters in the final inversion is composed from the diagonal elements of the correlation posterior covariance matrix. In this way cross-correlation information of the correlated parameters between the different locations is neglected. The former is probably more serious than the latter but it is beyond the scope of this paper to quantify the actual loss. As the theoretical examples show, the lateral parameter correlation method has the desired effect so it may tentatively be accepted that the cross-correlation information between the model parameters of the individual inversions is of minor importance compared with the variances.

The three steps of the lateral parameter correlation method can be seen as the first steps of an infinite iterative procedure that alternates between data inversion and correlation. However, numerical experiments indicate that there is no significant gain in going beyond the first three steps used here.

The theoretical examples demonstrated that extreme models from the first 1D data inversion can affect the lateral parameter correlation result. If, for example, the parameters of a certain layer are subject to equivalence, then, due to data errors, the layer thickness can become extremely thin or extremely thick. In the first case, the uncertainty of the thickness is very large so the thickness will not affect the correlation very much, i.e., the value of the thickness after the correlation

procedure will be determined by the values of the parameter at neighbouring soundings and the lateral smoothness constraint. If, on the other hand, the layer becomes thick, its uncertainty can become relatively small and the erroneously thick layer will influence its neighboring soundings in an undesired way. However, other methods of lateral correlation will have the same problem if it is caused by data errors, dimensionality effects or an insufficient noise description.

Only examples involving electrical and electromagnetic methods have been shown in this paper but evidently, the LPC method may be attractive also in other contexts of pointwise 1D inversion of massive data sets.

CONCLUSIONS

The lateral parameter correlation method is a fast and robust method of obtaining laterally smooth model sections from 1D inversion that will still fit the data. Even though covariance information between the model parameters is neglected, the lateral parameter correlation procedure works satisfactorily and does in fact impose lateral continuity between the model parameters in a proper way and without artefacts: well determined parameters have more influence than more poorly determined parameters. The method offers a posterior variance estimate of the parameters of the final inversion.

The lateral parameter correlation method is simple and involves only a few large-scale inversions. It is thus much faster than methods where all sounding data are inverted simultaneously, in typical applications by a factor of 200–400. For very large data sets the non-sparse LPC inversions can be segmented by considering overlapping intervals. The correlation formulation of the LPC method is the same for correlation along profile lines and correlation in the plane and thus avoids cumbersome selection criteria sometimes found in other formulations.

The final result does to some extent depend on extreme models from the individual inversions and the lateral parameter correlation method thus accentuates the demand for a good noise model and a well-defined inversion for the individual inversions.

It is easy to combine models from different EM methods and also to incorporate information from other sources (resistivity logs, layer boundaries from drill holes, etc.) as long as it can be formulated in terms of a 1D model.

ACKNOWLEDGEMENTS

We thank Bo Holm Jacobsen for fruitful discussion about the nature of the lateral parameter correlation method and for the

'geology-simulator' that generated the 2D test model for the theoretical example. The efforts of colleagues doing internal review are much appreciated.

REFERENCES

- Albouy Y., Andrieux P., Rakotondraso G., Ritz M., Descloitres M., Join J.-L. and Rasolomanana E. 2001. Mapping coastal aquifers by joint inversion of DC and TEM soundings: Three case histories. *Ground Water* **39**, 87–97.
- Auken E. and Christiansen A.V. 2004. Layered and laterally constrained 2D inversion of resistivity data. *Geophysics* **69**, 752–761.
- Auken E., Christiansen A.V., Jacobsen B.H., Foged N. and Sørensen K.I. 2005. Piecewise 1D laterally constrained inversion of resistivity data. *Geophysical Prospecting* **53**, 497–506. doi:10.1111/j.1365-2478.2005.00486.x
- Auken E., Pellerin L., Christensen N.B. and Sørensen K. 2006. A survey of current trends in near-surface electrical and electromagnetic methods. *Geophysics* **71**, G249–G260.
- Balch S., Boyko W., Black G. and Pedersen R. 2002. Mineral exploration with the AeroTEM system. 72nd SEG meeting, Salt Lake City, Utah, USA, Expanded Abstracts, 9–12.
- Bernstone C. and Dahlin T. 1999. Assessment of two automated DC resistivity data acquisition systems for landfill location surveys: Two case studies. *Journal of Environmental and Engineering Geophysics* **4**, 113–121.
- Brodie R. and Sambridge M. 2006. A holistic approach to inversion of frequency-domain airborne EM data. *Geophysics* **71**, G301–G312.
- Dahlin T. 1996. 2D resistivity surveying for environmental and engineering applications. *First Break* **14**, 275–283.
- Eaton P., Anderson B., Nilsson B., Lauritsen E., Queen S. and Barnett C. 2002. NEWTEM - A novel time-domain helicopter electromagnetic system for resistivity mapping. 72nd SEG meeting, Salt Lake City, Utah, USA, Expanded Abstracts, 1–4.
- Edwards L.S. 1977. A modified pseudosection for resistivity and IP. *Geophysics* **42**, 1020–1036.
- Farquharson C.G. and Oldenburg D.W. 1998. Non-linear inversion using general measures of data misfit and model structure. *Geophysical Journal International* **134**, 213–227.
- Fitterman D.V. 1987. Examples of transient sounding for groundwater exploration in sedimentary aquifers. *Groundwater* **25**, 684–693.
- Gyulai Á and Ormos T. 1999. A new procedure for the interpretation of VES data: 1.5-D simultaneous inversion method. *Journal of Applied Geophysics* **64**, 1–17.
- Inman J.R. Jr, Ryu J. and Ward S.H. 1975. Resistivity inversion. *Geophysics* **38**, 1088–1108.
- Loke M.H., Acworth I. and Dahlin T. 2003. A comparison of smooth and blocky inversion methods in 2-D electrical imaging surveys. *Exploration Geophysics* **34**, 182–187.
- Loke M.H. and Barker R.D. 1996. Rapid least-squares inversion of apparent-resistivity pseudosections by a quasi-Newton method. *Geophysical Prospecting* **44**, 131–152. doi:10.1111/j.1365-2478.1996.tb00142.x
- McGillivray P.R. 1992. *Forward modeling and inversion of DC resistivity and MMR data*. PhD thesis, The University of British Columbia, Vancouver, Canada.
- Menke W. 1989. *Geophysical Data Analysis: Discrete Inversion Theory*. Academic Press. ISBN 0124909213.
- Møller I., Jacobsen B.H. and Christensen N.B. 2001. Rapid inversion of 2-D geoelectrical data by multichannel deconvolution. *Geophysics* **66**, 800–808.
- Olayinka A.I. and Yaramanci U. 2000. Use of block inversion in the 2-D interpretation of apparent resistivity data and its comparison with smooth inversion. *Journal of Applied Geophysics* **45**, 63–81.
- Oldenburg D.W. and Li Y. 1994. Inversion of induced polarization data. *Geophysics* **59**, 1327–1341.
- Panissod C., Lajarthe M. and Tabbagh A. 1997. Potential focusing: a new multi-electrode array concept, simulating study, and field tests in archaeological prospecting. *Geophysics* **38**, 1–23.
- Sandberg S.K. and Hall D.W. 1990. Geophysical investigation of an unconsolidated coastal plain aquifer system and the underlying bedrock geology in Central New Jersey. In: *Geotechnical and Environmental Geophysics Vol. 1* (ed. S.H. Ward), pp. 311–320. SEG. ISBN 0931830990.
- Santos F.A.M. 2004. 1-D laterally constrained inversion of EM34 profiling data. *Journal of Applied Geophysics* **56**, 123–134.
- Sengpiel K.-P. and Siemon B. 2000. Advanced inversion methods for airborne electromagnetic exploration. *Geophysics* **65**, 1983–1992.
- Serban D.Z. and Jacobsen B.H. 2001. The use of broadband prior covariance for inverse palaeoclimate estimation. *Geophysical Journal International* **147**, 29–40.
- Siemon B. 2001. Improved and new resistivity-depth profiles for helicopter electromagnetic data. *Journal of Applied Geophysics* **46**, 65–76.
- Smith J.T., Hoversten M., Gasperikova E. and Morrison F. 1999. Sharp boundary inversion of 2D magnetotelluric data. *Geophysical Prospecting* **47**, 469–486. doi:10.1046/j.1365-2478.1999.00145.x
- Sørensen K.I. 1996. Pulled array continuous electrical profiling. *First Break* **14**, 85–90.
- Sørensen K.I. and Auken E. 2004. SkyTEM - A new high-resolution helicopter transient electromagnetic system. *Exploration Geophysics* **35**, 191–199.
- Sørensen K.I., Auken E., Christensen N.B. and Pellerin L. 2005. *An Integrated Approach for Hydrogeophysical Investigations: New Technologies and a Case History*. SEG.
- Taylor K., Widmer M. and Chesley M. 1992. Use of transient electromagnetics to define local hydrogeology in an arid alluvial environment. *Geophysics* **57**, 343–352.
- Tezkan B. 1999. A review of environmental applications of quasi-stationary electromagnetic techniques. *Surveys in Geophysics* **20**, 279–308.
- Tezkan B., Hördt A. and Gobashy M. 2000. Two dimensional inversion of radiomagnetotelluric data: selected case histories for waste site exploration. *Journal of Applied Geophysics* **44**, 237–256.
- Tølbøll R.J. 2007. *Application of frequency domain helicopterborne electromagnetic methods for hydrogeological investigations in Denmark*. PhD thesis, Department of Earth Sciences, University of Aarhus.
- Tølbøll R.J. and Christensen N.B. 2006. Robust 1D inversion and analysis of helicopter electromagnetic (HEM) data. *Geophysics* **71**, G53–G62.